Theoretical Thermal Model of MIG Welding of FSS (AISI 430) Using ANSYS and Its Experimental Verification

Md Razaullah Khan[1], A. K. Pathak[2] and Sree Harsha Ch[3]
[1]Ph. D. Scholar, NIFFT, Hatia, Ranchi, 834003, Email: myrunni@gmail.com
[2]Professor, NIFFT, Hatia, Ranchi, 834003, Email: ajaipathak@yahoo.com,
[3]M. Tech. Student, NIFFT, Hatia, Ranchi, 834003, Email: sreeharshachoutapalli@gmail.com

DOI :10.22486/iwj/2018/v51/i3/175003

ABSTRACT

Metallurgical and mechanical properties of a weldment depend on its cooling rate and temperature distribution during welding. Temperature distribution and cooling rate are responsible for formation of different microstructures and different size of grain in different zones. If cooling rate and temperature distribution can be predicted in advance it will help the design engineer at the design stage itself to design a good welded joint. Determination of cooling rate and temperature distribution in welding experimentally is very costly and time taking. In this work the cooling rate and temperature distribution was theoretically predicted using ANSYS14 and experimentally verified. For the theoretical thermal analysis, 3D modeling of thermal simulation of arc welding (MIG) process was done by using ANSYS14. The special feature of the analysis is the use of a fast iterative procedure during a single pass welding. Temperature dependent metal properties of AISI 430 were taken from standard data source and were utilized till to the liquid phase. Element shape '3-D 10-Node tetrahedral' (solid 87) was used in 3-D analysis. Conduction and convection are considered as heat transfer mode. The experimental values of welding speed, welding current, and arc voltage were used for theoretical analysis. Thermocouples were used to record welding temperature using data tracker and computer. Five thermocouples were fixed at the middle line of the plate to measure temperature distribution and cooling rate practically. Two plates of FSS were welded by MIG welding in butt joint position in single pass.

KEYWORDS: Ferritic stainless steel; MIG welding; Cooling rate; Temperature distribution; Thermocouple; ANSYS.

1.0 INTRODUCTION

Ferritic stainless steels are iron-chromium alloys having chromium content usually in the range of 10.5–27 %. In these steels the predominant metallurgical phase present is ferrite. These steels are Fe-Cr-C alloys with sufficient chromium or chromium plus other ferrite stabilizer, such as aluminium, niobium, molybdenum, or titanium, and are used to inhibit the formation of austenite on heating. They are used in a variety of application where corrosion resistance rather than mechanical properties (strength, toughness and ductility), is the primary service requirements. Low chromium (10.5-12.5 wt%) grades are used for application such as automotive exhaust system, where resistance to general corrosion is superior to carbon steels. Medium and high chromium grades are used in more aggressive corrosion environments. High chromium grades are also used in high efficiency furnaces [1]. The annealed ferritic stainless steels containing 16% to 18% Cr offer acceptable oxidation and corrosion resistance in many environments. The ferritic stainless steels are generally considered to have poor weldability when compared to the austenitic stainless steels and their mechanical properties and corrosion resistance are adversely affected by welding. Ferritic stainless steel is a

candidate material in less severe corrosion atmosphere for chemical processing equipment, furnace parts, and heat exchangers, petroleum refining equipment, storage vessels, electrical appliances, solar water heaters, and household appliances. They are particularly more appropriate in caustic and chloride environments. However, despite these economic and metallurgical attributes, the ferritic stainless steels are less used in engineering application. This is because fusion welding of ferritic stainless steel particularly the first generation group (AISI 430, 442 and 446) is associated with many problems such as grain growth in both the fusion zone and HAZ and formation of martensite at the grain boundary in the weld zone which may affect the ductility and toughness of the weldment.

Many researchers have worked on FEM model of arc welding. Here works of some of the researchers have been presented as literature survey. P. Tekriwal et al. have done three dimensional finite element analysis of transient heat transfer in GMA Welding. The finite element model was used to predict weld metal zone and heat affected zone. The predicted values were experimentally verified [2]. Vineet Negi et al. have solved the FEM model by assuming double-ellipsoidal with Gaussian volumetric heat generation during SAW. Model was solved by ANSYS12. The temperature distribution was predicted at some distance away from the weld line. Temperature of plate during welding was measured experimentally using infrared thermography. It was found that experimental results well corresponds to the results predicted by ANSYS [3]. Kumar KS has analyzed a three dimensional finite element technique using comsol code to simulate the welding process for two different laser spot positions. Thermal profile, isothermal surface, and deformation of the dissimilar joints were simulated to investigate the temperature distribution across the butt joints. The experimental and predicted results exposed the bead width and heat affected zone in dissimilar joints were compared and found very close association with each other [4]. Theoretical investigation of heat transfer in welding of FSS is not available in literature therefore, in the present work author have investigated the welding heat transfer in FSS using ANSYS. The main objective of this work was to study the theoretical thermal analysis of MIG welding process using ANSYS and its experimental verification.

2.0 EXPERIMENTAL MEASUREMENT OF TEMPERATURE DISTRIBUTION AND COOLING RATE

Fig. 1 shows the geometry of two FSS plates in butt welding position. One plate of 320 mm × 100 mm × 3 mm of ferritic stainless steel was taken to fix thermocouples. Five blind holes from the welding edge at the distance of 4 mm, 9 mm, 14 mm, 20 mm, and 27 mm i.e at point a, b, c, d, and e respectively were drilled using 3 mm drill bit at the middle of the plate i.e. at 160 mm in direction of length. Five K type thermocouples were brazed in these holes as shown in **Fig. 2**. The heat transfer due to welding will be uniformly distributed in both the plates and will have similar pattern. Therefore for the sake of simplicity only one plate was considered for analysis. These thermocouples were attached to 8-pin data tracker. This data tracker was attached to computer through connecting wire. The variation of temperature was verified using controlled heating. In **Fig. 2**, t = 0 s is the starting time of welding, t = 21 s is the time when arc reaches the centre of plate (in the line of thermocouple) and t = 41 s is the finishing time of welding. The welding was completed in single pass by MIG welding using mixture of argon and 2% oxygen as shielding gas, having full penetration. Variation of voltage and current with respect to time was recorded during welding. Mean value of current and voltage was calculated for analysis. The welding speed was calculated from the finishing time of welding and length of the weld. Experimental welding parameters are recorded in **Table 1**. Temperature of plate was recorded in computer through data tracker continually with respect to time. The temperature was recorded till the plates cool to the room temperature. Data recorded was used to plot temperature distribution curve and cooling curve using excel. **Fig. 3** shows the set up of plate with thermocouple attached to base metal, and **Fig. 4** shown the plate after welding with used thermocouple.

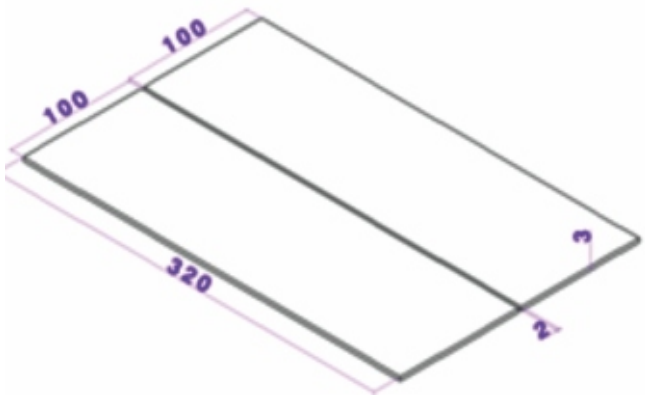

Fig. 1 : Butt weld setup of FSS plate.

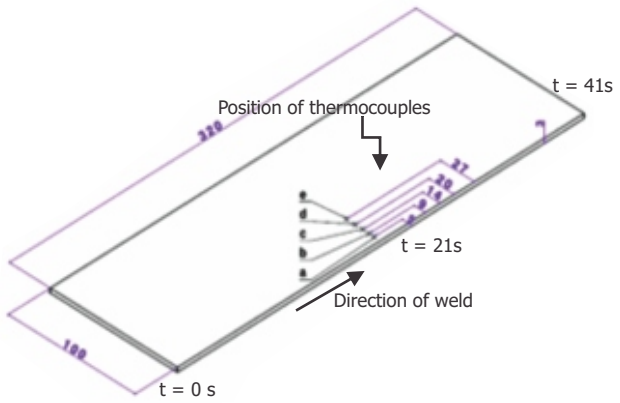

Fig. 2 : Geometry of plate with position of thermocouples.

Fig. 4 : Plate after welding with thermocouple

Table 1 : Welding process parameters

Process	MIG, DCEP, full penetration weld
Position	Horizontal / flat
Welding current	213.24 A (average value)
Welding voltage	14.89 V (average value)
Welding Speed	7.8 mm/s
Wire electrode	Austenitic stainless steel filler material (ER309L)
Electrode stick out	9.5 -10 mm
Electrode feed rate	5.8 m/min = 96.66 mm/sec
Torch position	Vertical
Upper shielding	Mixture of argon and 2% oxygen
Shielding gas flow rate	6 l/min
Underneath shielding	None, instead supported on a refractory brick

Fig. 3 : Setup of plate in welding position

3.0 THERMAL MODEL

3.1. Materials properties

Material properties required for thermal analysis in welding are thermal conductivity, density, specific heat and enthalpy. Temperature dependent thermal conductivity, specific heat and density were considered for the analysis. The value of enthalpy was calculated from specific heat. The material used in this study was 3 mm thick cold rolled AISI 430 ferritic stainless steel plate and filler wire electrode ER309L (ASS).

Enthalpy = ρ c (t - t_o), Where t = Temperature of work piece, t_o = Room temperature 298.5 K, ρ = Density (kg/m^3), c = Specific heat (J/(kg K).

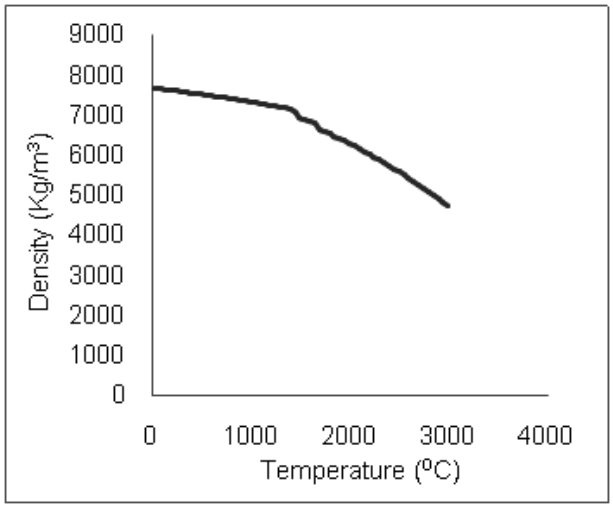

Fig. 5 : Variation of density of AISI 430 with temperature.

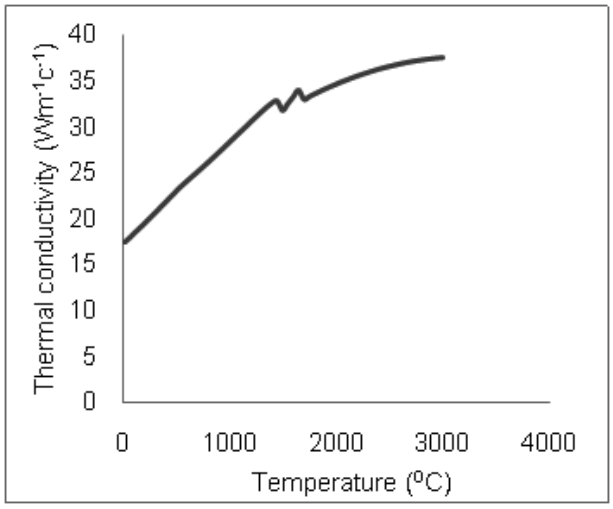

Fig. 6 : Variation of thermal conductivity of AISI 430 with temperature.

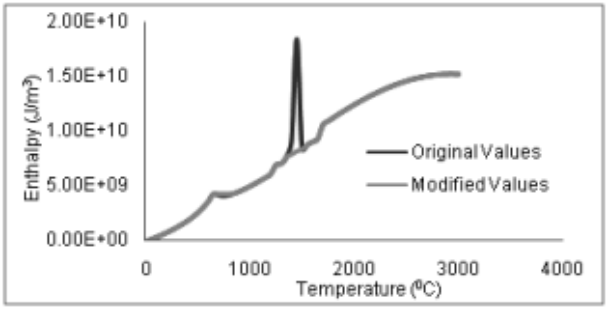

Fig. 7 : Variation of calculated and modified values of enthalpy of AISI 430.

Fig. 5 and **Fig. 6** show the variation of density and thermal conductivity respectively, of AISI 430 FSS with respect to temperature [5]. ANSYS was run with the calculated value of enthalpy as shown in **Fig. 7**. Due to sharp changes in value of enthalpy at some points ANSYS was showing errors. Hence, to make the data compitable with ANSYS graph was smoothen at the required points and ANSYS was excuited with the modified values.

3.2 Required data used in the thermal model

Calculation of no of steps: Let 3.2 mm is the arc radius, Length of plate = 320 mm,

Total number of steps = 320/6.4= 50

Time interval calculation

Total time taken in welding = 41 second, i.e 50 steps were made in 41 second.

So time taken for 1 step = 41/50 = 0.82 s

Heat flux calculation

Heat input = $V_{avg} \times I_{avg}$, = 14.89 × 213.24 = 3175.1436 W

Taking arc efficiency, η = 0.80 [6]

Therefore, net heat transfer rate = η × heat input = 0.80 × 3175.1436 = 2540.1148 W

Area of one circle = $\pi r^2 = 3.141 \times 0.0032^2 = 3.216 \times 10^{-5}$ m^2

$$\text{Heat flux} = \frac{\text{net heat input}}{\text{area of circle}} = \frac{2540.1148}{3.216 \times 10^{-5}} = 7.89 \times 10^7 \text{ W/m}^2$$

Heat flux on each semicircle = 7.89 x 10^7 W/m^2

Heat flux on each quarter circle = 7.89 x 10^7 W/m^2

Convective heat transfer coefficient acting on the top surface of the plate [7]: h = 35 W/m^{2}K

3.3. Thermal analysis by ANSYS

Thermal analysis was done with the help of ANSYS 14.5. Three dimensional model of plate was prepared. Arc efficiency was considered equal to 80% [6] hence; radiation effect was not considered. Convection heat transfer (h = 35 W/m^{2}K) was considered on the top surface of the plate. **Fig. 8** shows the variation of convective heat transfer coefficient with velocity [7]. SOLID 87 element shown in **Fig. 9** was used for finite element analysis. SOLID 87 10-Node Tetrahedral Thermal Solid or SOLID 87 is well suited to model irregular meshes (such as produced from various CAD/CAM systems) [8].

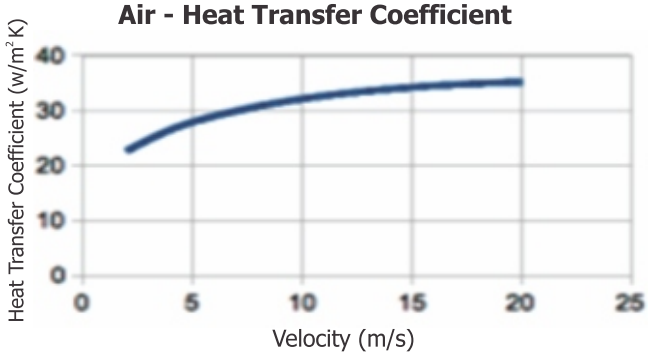

Fig. 8 : Air heat transfer coefficient with velocity [7].

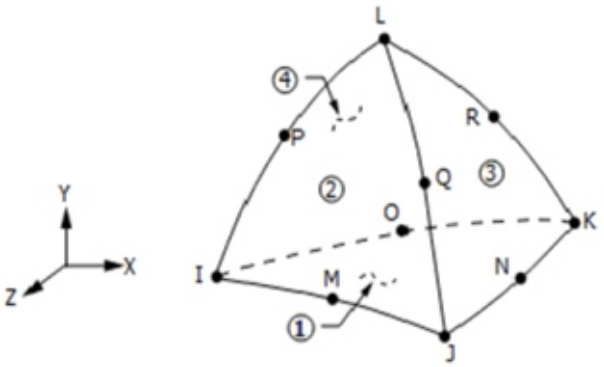

Fig. 9 : 10-Node Tetrahedral thermal solid (SOLID87)

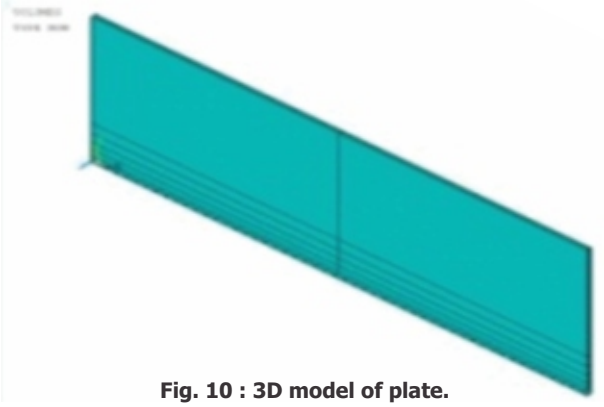

Fig. 10 : 3D model of plate.

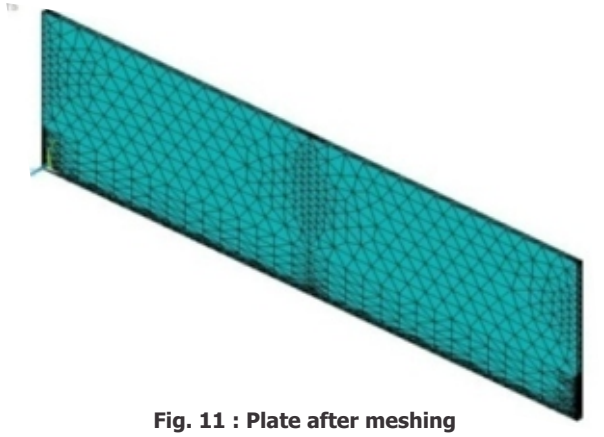

Fig. 11 : Plate after meshing

Fig. 10 shows the 3D model of plate with semicircles made based on welding speed. The semicircle on the plate represents the position of arc in a particular step. **Fig. 11** shows the 3D model of plate in mesh. Heat flux was assumed to be uniformly distributed on a circular spot. Arc diameter was taken equal to the bead diameter. Heat flux of 7.89×10^7 W/m^2 was applied on each semicircle and quarter circle (in beginning and last). Convection heat transfer was considered on top surface of the plate including semicircles. Since it is a non linear transient analysis Newton Raphson method was activated. Heat flux was first applied on quarter circle and then it was moved to semicircle in steps by using KBC,1 command prior to start the solution. Heat flux was moved from one semicircle to another at regular interval of 0.82 sec. One step was solved in 20 iterations using its command for convergence. The simulation was done for 600 sec. Thus problem was solved by ANSYS and results were recorded in post processor. Different curves were drawn from the result.

4.0 RESULTS AND DISCUSSIONS

4.1 Cooling Curve

Data were recorded from theoretical analysis and practical results to plot cooling curve at different points. Cooling curves for experimental and theoretical value are shown in **Fig. 12** to **Fig. 16** for thermocouple positions a, b, c, d and e respectively. Temperature rise takes place in workpiece due to conduction and with lapse of time temperature falls due to conduction and convection both.

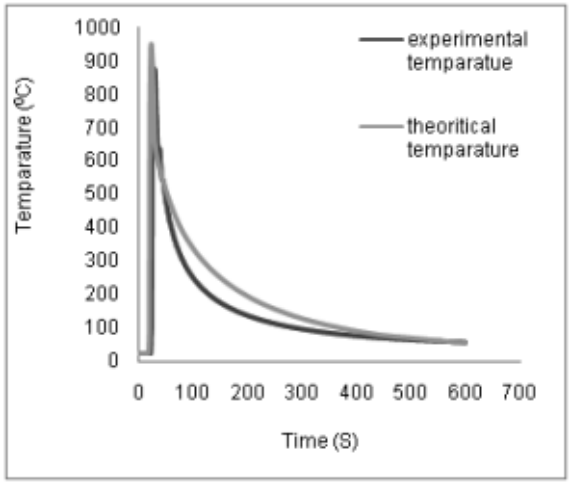

Fig. 12 : Experimental and theoretical cooling curves at point 'a'.

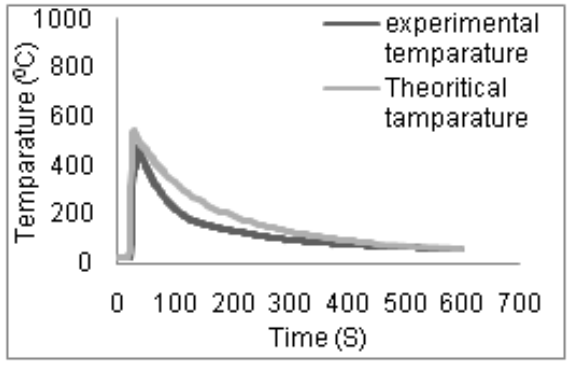

Fig. 13 : Experimental and theoretical cooling curves at point 'b'.

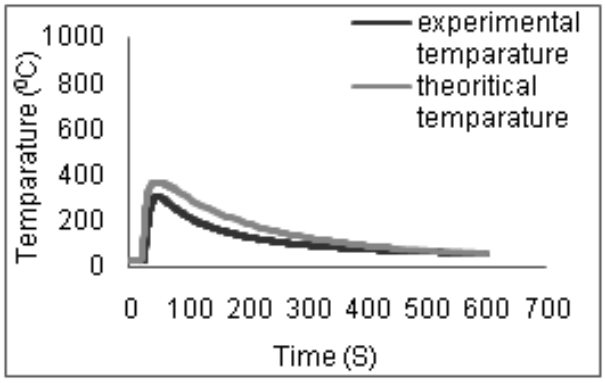

Fig. 14 : Experimental and theoretical cooling curves at point 'c'.

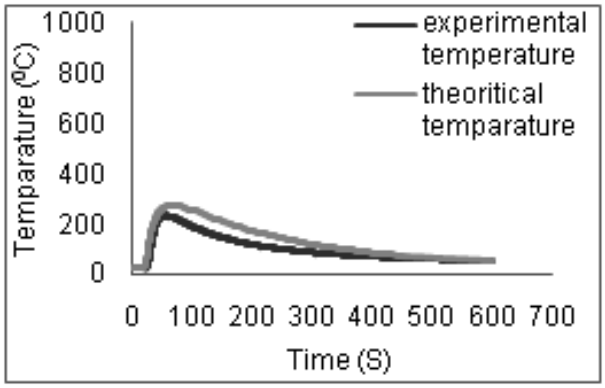

Fig. 15 : Experimental and theoretical cooling curves at point 'd'.

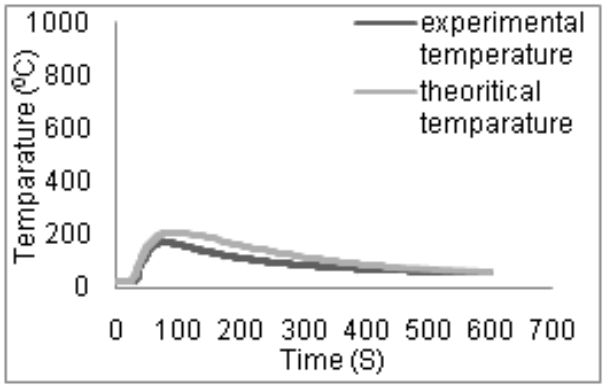

Fig. 16 : Experimental and theoretical cooling curves at point 'e'.

Fig. 12 to 16 compare the experimental and theoretical cooling curves at point a, b, c, d and e (refer **Fig. 2**). It can be seen that theoretical cooling curve and experimental cooling curve show the same temperature pattern with some deviation.

4.2 Temperature Distribution Curves

Temperature distribution curves were plotted for both experimentally measured values and theoretically estimated values at different instant of time in **Fig. 17 to 19**.

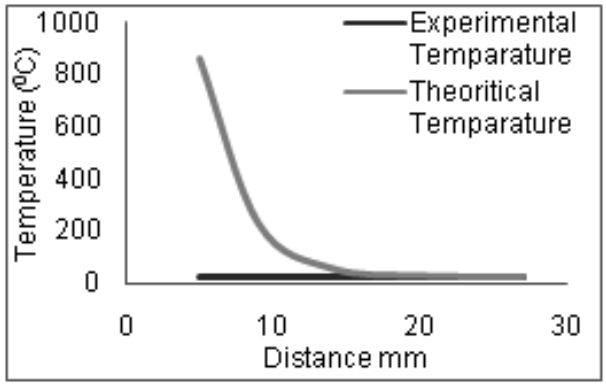

Fig. 17 : Temperature distribution curves at 21 s

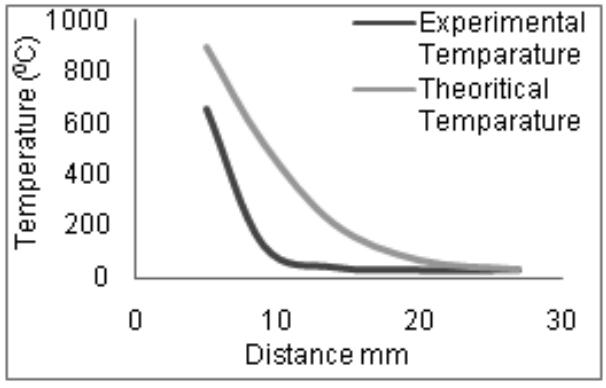

Fig. 18 : Temperature distribution curves at 25 s

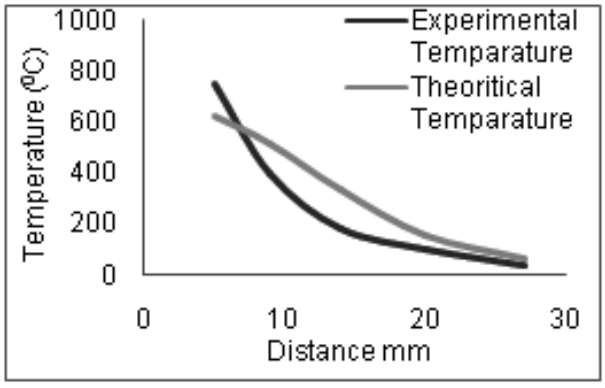

Fig. 19 : Temperature distribution curves at 32 s

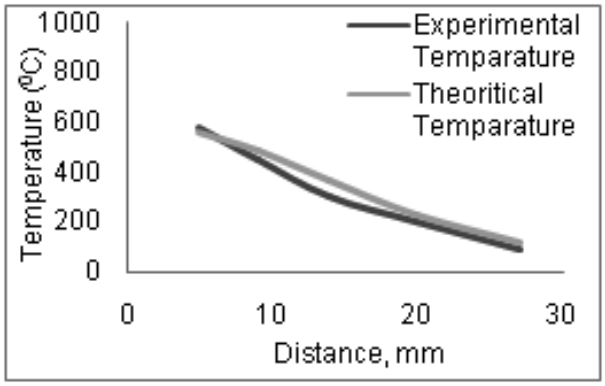

Fig. 20 : Temperature distribution curves at 41 s

Fig. 17 to 20 compare experimental and theoretical temperature distribution at point a, b, c, d, e at t = 21 s, 25 s, 32 s, and 41 s. **Fig. 17** show temperature distributions when arc is at centre line of the plate. It can be seen that there is no temperature rise in the thermocouple at this point. This happens because thermocouple takes some time to record the temperature. It depends on the sensitivity of the thermocouple. Hence recorded temperature lags behind the temperature rise predicted by ANSYS. **Fig. 18** shows that due to poor sensitivity of thermocouple the temperature recorded by thermocouple lags behind the temperature recorded by the ANSYS. After elapse of longer duration of time (**Fig. 19** and **Fig. 20**) the experimental temperature distribution match with the theoretical temperature distribution with small deviation. In all the cases the pattern of temperature distribution is same in both the cases. **Fig. 20** shows that the experimental and theoretical temperature distribution well mach with each other.

4.3 Temperature contour plots on plate at different instant of time

Temperature contour plot on plate obtained from ANSYS are shown in **Fig. 21** and **Fig. 22** at time t = 25 s and t = 32 s respectively. Similarly the temperature contour plot can be obtained at different time. With the lapse of time, due to conduction temperature increases across the plate.

5.0 CONCLUSIONS

1. Theoretical and practical temperature distributions at the centre line of plate along the width were compared at different instant of welding time. It was observed that the temperature distribution pattern for theoretical values and experimental values are the same, with some deviation.

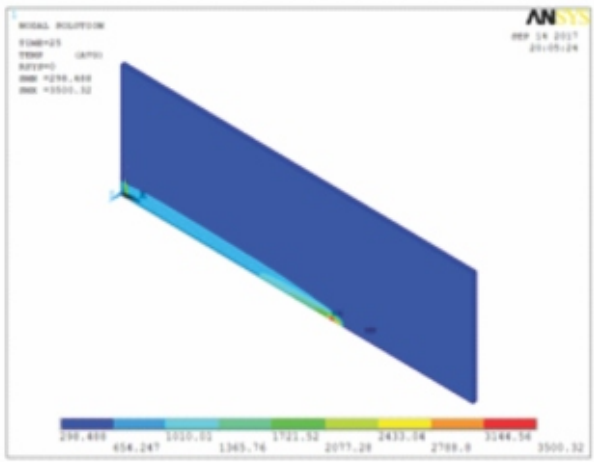

Fig. 21 : Temperature contour plot on plate at 25 s

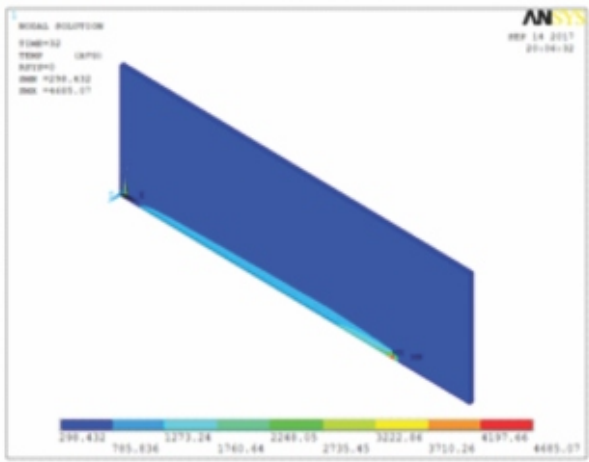

Fig. 22 : Temperature contour plot on plate at 32 s

2. The cooling curves at different points were drawn for theoretical value and practical values. It was observed that the theoretical cooling curve and the experimental cooling curve shows same pattern with some deviation.
3. The deviation comes due to poor sensitivity of the thermocouple and some inherent practical error. Thermocouple reading was also affected due to welding current. Some deviation may come due to approximation used in modeling of the ANSYS.
4. Patterns of temperature distribution obtained from ANSYS for different position of arc and at different time match well with the pattern reported in literature [9-11].
5. It can be concluded that the theoretical thermal model discussed in the paper can be used to predict the temperature distribution and cooling rate in weldment with reasonable accuracy.

ACKNOWLEDGMENT

The present paper is a revised version of an article presented in the International Congress (IC-2017) of the International Institute of Welding held in Chennai on December 07-09, 2017, and organized by the Indian Institute of Welding.

REFERENCES

[1] Lippold JC and Kotecki DJ (2005); Welding Metallurgy and Weldability of Stainless Steels, John Wiley and Sons, p.87.

[2] Tekriwal P and Mazumder J (1988); Finite element analysis of three-dimensional transient heat transfer in GMA welding, Welding Journal, Research and Development, pp.150s-156s.

[3] Negi V and Chattopadhyaya S (2013); Critical assessment of temperature distribution in submerged arc welding process, Advances in Materials Science and Engineering, Article ID 543594, pp.1-9.

[4] Kumar KS (2015); Investigation on transient thermal responses on 316L austenitic stainless steel and low carbon ferritic steel welding using pulsed Nd: YAG laser, Material Science & Engineering, 4(6), pp.1-9.

[5] Ho GY and Chu TK (1977); Electrical resistivity and thermal conductivity of nine selected AISI stainless steels, CINDAS Report 45, Prepared by American Iron and Steel Institute, p.37.

[6] ASM Handbook (1993); vol. 6, ASM International, p.71.

[7] http://www.engineeringtoolbox.com/convective-heat-transfer-d_430.html

[8] ANSYS 14.5 Help Desk Element Type.

[9] Pathak AK and Datta GL (1999); Three-dimensional finite element analysis of heat flow in arc welding, Indian Welding Journal, 32(3), pp.32-38.

[10] Silva PN and Narayanan Sankar TK (1996); Finite element analysis of temperature distribution during arc welding using adaptive grid technique, Welding Journal, 75(4), pp. 123s-128s.

[11] Ismail MIS and Afieq WM (2016); Thermal analysis on a weld joint of aluminium alloy in gas metal arc welding, Advances in Production Engineering and Management, 11(1), pp.29-37.